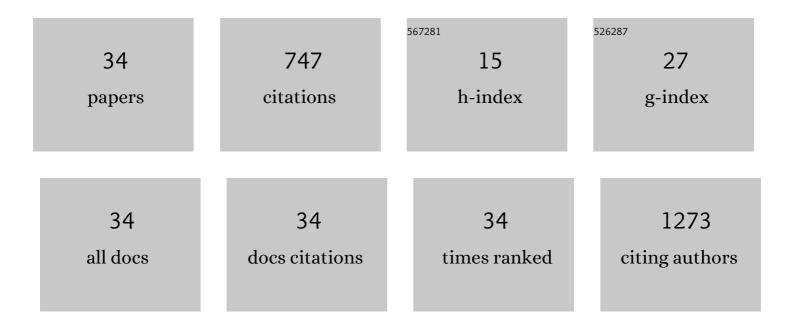
Ying Zhou

List of Publications by Year in descending order

Source: https://exaly.com/author-pdf/201832/publications.pdf Version: 2024-02-01



YINC 7HOU

#	Article	IF	CITATIONS
1	Highly-efficient and easy separation of γ-Fe2O3 selectively adsorbs U(Ⅵ) in waters. Environmental Research, 2022, 210, 112917.	7.5	17
2	Incorporation of lead into pyromorphite: Effect of anion replacement on lead stabilization. Waste Management, 2022, 143, 232-241.	7.4	2
3	Single-molecule brightness analysis for the determination of anticancer drug interactions with DNA. Analyst, The, 2020, 145, 6600-6606.	3.5	6
4	Pb Stabilization by a New Chemically Durable Orthophosphate Phase: Insights into the Molecular Mechanism with X-ray Structural Analysis. Environmental Science & Technology, 2020, 54, 6937-6946.	10.0	7
5	Highly conducting, durable and large area carbon nanotube thick films for stretchable and flexible electrodes. Applied Physics Letters, 2019, 114, .	3.3	9
6	A highly durable, stretchable, transparent and conductive carbon nanotube–polymeric acid hybrid film. Nanoscale, 2019, 11, 3804-3813.	5.6	43
7	Fluorescence correlation spectroscopy for multiple-site equilibrium binding: a case of doxorubicin–DNA interaction. Physical Chemistry Chemical Physics, 2019, 21, 1572-1577.	2.8	20
8	Effectively immobilizing lead through a melanotekite structure using low-temperature glass-ceramic sintering. Dalton Transactions, 2019, 48, 3998-4006.	3.3	7
9	Highly crystalline lithium chloride-intercalated graphitic carbon nitride hollow nanotubes for effective lead removal. Environmental Science: Nano, 2019, 6, 3324-3335.	4.3	16
10	Nonuniform functional group distribution of carbon nanotubes studied by energy dispersive X-ray spectrometry imaging in SEM. Nanoscale, 2019, 11, 21487-21492.	5.6	11
11	Combined Fe ₂ O ₃ and CaCO ₃ Additives To Enhance the Immobilization of Pb in Cathode Ray Tube Funnel Class. ACS Sustainable Chemistry and Engineering, 2018, 6, 3669-3675.	6.7	7
12	Stable iodide doping induced by photonic curing for carbon nanotube transparent conductive films. Japanese Journal of Applied Physics, 2018, 57, 065101.	1.5	3
13	Structures and Fluorescence Properties for the Crystals, Powders, and Thin Films of Dithienylhexatrienes: Effects of Positional Isomerism. Crystal Growth and Design, 2018, 18, 6477-6487.	3.0	5
14	Lead removal from water – dependence on the form of carbon and surface functionalization. RSC Advances, 2018, 8, 18355-18362.	3.6	36
15	Epitaxial Growth of C ₆₀ on Rubrene Single Crystals for a Highly Ordered Organic Donor/Acceptor Interface. Crystal Growth and Design, 2017, 17, 4622-4627.	3.0	17
16	Constructing Nanostructured Donor/Acceptor Bulk Heterojunctions via Interfacial Templates for Efficient Organic Photovoltaics. ACS Applied Materials & Interfaces, 2017, 9, 43893-43901.	8.0	5
17	Mineralization of perfluorooctanesulfonate (PFOS) and perfluorodecanoate (PFDA) from aqueous solution by porous hexagonal boron nitride: adsorption followed by simultaneous thermal decomposition and regeneration. RSC Advances, 2016, 6, 113773-113780.	3.6	20
18	Carbon nanotube based transparent conductive films: progress, challenges, and perspectives. Science and Technology of Advanced Materials, 2016, 17, 493-516.	6.1	125

Үімд Хнои

#	Article	IF	CITATIONS
19	Fabrication of carbon nanotube hybrid films as transparent electrodes for small-molecule photovoltaic cells. RSC Advances, 2016, 6, 25062-25069.	3.6	10
20	Understanding the doping effects on the structural and electrical properties of ultrathin carbon nanotube networks. Journal of Applied Physics, 2015, 118, 215305.	2.5	15
21	Building interconnects in carbon nanotube networks with metal halides for transparent electrodes. Carbon, 2015, 87, 61-69.	10.3	24
22	Understanding Device-Structure-Induced Variations in Open-Circuit Voltage for Organic Photovoltaics. ACS Applied Materials & Interfaces, 2015, 7, 10814-10822.	8.0	2
23	Morphological analysis of co-evaporated blend films based on initial growth for organic photovoltaics. Applied Surface Science, 2015, 355, 1261-1266.	6.1	1
24	Efficient small-molecule photovoltaic cells using nanostructured template. Proceedings of SPIE, 2014,	0.8	1
25	Structural influences on charge carrier dynamics for small-molecule organic photovoltaics. Journal of Applied Physics, 2014, 116, 013105.	2.5	6
26	Efficient Smallâ€Molecule Photovoltaic Cells Using a Crystalline Diindenoperylene Film as a Nanostructured Template. Advanced Materials, 2013, 25, 6069-6075.	21.0	39
27	Structural modifications of zinc phthalocyanine thin films for organic photovoltaic applications. Journal of Applied Physics, 2012, 111, .	2.5	13
28	Phase separation of co-evaporated ZnPc:C60 blend film for highly efficient organic photovoltaics. Applied Physics Letters, 2012, 100, 233302.	3.3	50
29	Glancing Angle Deposition of Copper Iodide Nanocrystals for Efficient Organic Photovoltaics. Nano Letters, 2012, 12, 4146-4152.	9.1	92
30	Size and shape controlled LiMnPO4 nanocrystals by a supercritical ethanol process and their electrochemical properties. Journal of Materials Chemistry, 2011, 21, 15813.	6.7	74
31	Controlled growth of dibenzotetraphenylperiflanthene thin films by varying substrate temperature for photovoltaic applications. Solar Energy Materials and Solar Cells, 2011, 95, 2861-2866.	6.2	20
32	Improved Dielectric Properties of Tetragonal ZrO2Gate Dielectric Fabricated by Ozone-Assisted Sputtering. Japanese Journal of Applied Physics, 2009, 48, 060208.	1.5	3
33	The modifications of the surface wettability of amorphous carbon films. Colloids and Surfaces A: Physicochemical and Engineering Aspects, 2009, 335, 128-132.	4.7	24
34	SUPERHYDROPHOBIC SURFACES PREPARED BY PLASMA FLUORINATION OF LOTUS-LEAF-LIKE AMORPHOUS CARBON FILMS. Surface Review and Letters, 2006, 13, 117-122.	1.1	17